Original Article

Adsorption potential for PM$_{2.5}$ and TVOC from printing job using wastepaper and rice husk

Nanthana Chanthorn[1], Thanathorn Petchrat[1], Titiwud Pongtanapaisan[1],
Sirikarn Thongmai[1], and Thanakrit Neamhom[1, 2*]

*[1] Department of Environmental Health Sciences, Faculty of Public Health,
Mahidol University, Ratchathewi, Bangkok, 10400 Thailand*

*[2] Center of Excellence on Environmental Health and Toxicology (EHT), Office of the Permanent Secretary,
Ministry of Higher Education, Science, Research and Innovation, Ratchathewi, Bangkok, 10400 Thailand*

Abstract

This study aimed to investigate the efficiency of aerogel adsorbent produced from combining wastepaper and rice husk to reduce printing pollutants. They were prepared from rice husk residue and three types of wastepaper including two sides-used paper (2P), color paper, and newspaper. In printing operation, the concentrations of PM$_{2.5}$ and TVOC were found at 0.019±0.005 mg/m^3 and 0.185±0.005 ppm, respectively. Factorial designs by eighteen experiments revealed the use of color and newspaper wastes resulted higher removal efficiency for PM$_{2.5}$ whereas the efficiency for TVOC differed compared with the 2P protocol. Moreover, applying 2P achieved better values for both emissions and provided the best aerogel obtained from 2P without pretreatment and proportion between rice husk and wastepaper at 1:1 (52.6 and 56.2% for PM$_{2.5}$ and TVOC, respectively). To determine adsorption behavior at equilibrium, the adsorption isotherms were fitted to the Langmuir equation with an R^2 value of 0.8201 and 0.9973 for PM$_{2.5}$ and TVOC, respectively. The adsorption sites on the aerogel surface were homogeneous in nature and presented a strong interaction between pollutants and adsorbent fibers. They revealed a maximum capacity for PM$_{2.5}$ and TVOC of 0.0008 mg/g and 0.099 ppm/g, respectively.

Keywords: PM$_{2.5}$, TVOC, aerogel, adsorption, wastepaper, rice husk

1. Introduction

Presently, humans spend more than 90% of their daily life indoors resulting in a growing demand for fresh, healthy, and comfortable indoor environments (Lee & Koo, 2015). By reason of environmental health, the regulations of Indoor Air Quality (IAQ) have been mentioned in various modern societies to prevent the occurrence of health illnesses and uncomfortable daily life activities (United State Environmental Protection Agency [US.EPA], 1997). They have become concerning issues to businesses, residents, and employees. Numerous scientific studies have revealed synergistic links between exposure to indoor pollutants for both solid and gaseous phases and health problems ranging from simple respiratory symptoms to morbidity and mortality (Chullasuk, Chapman, & Taneepanichskul, 2016; Gu & Karrasch, 2020). Printers have been frequently used as equipment in daily life and much evidence shows the potential risks as indoor pollutant sources (Shi *et al.*, 2015). He, Morawska, & Taplin (2007) investigated particle number and PM$_{2.5}$ emissions from printers in an office building and revealed that they emit particles in an ultrafine range. Not only PM$_{2.5}$ and other particulate matters, printers can also emit volatile organic compounds (VOC), ozone, ultraviolet light, and other carbon elements (Kagi, Fujii, Horiba, Namiki, & Ohtani, 2007; Lee, Dai, Chien, & Hsu, 2006).

Wastepaper products (WP) from printing mistakes, handouts, presentations, and packaging, make up an estimated 70% of the total waste in offices. WP is rich in cellulose fibers, which is particularly attractive as feedstock for many

*Corresponding author
Email address: nt.thanakrit@gmail.com

purposes due to growing recycling awareness and ready availability such as in biofuels (Guerfali, Saidi, & Gargouri, 2015; Li *et al*., 2020) and adsorptive materials productions (Li *et al*., 2018b; Lovskaya, Menshutina, Mochalova, & Nosov, 2020; Rinki, Dutta, Hunt, MacQuarrie, & Clark, 2011). Despite being composed of cellulose, hemicellulose, and lignin which are the main restricted components for absorbency (Kumar & Bandyopadhyay, 2006), many related researchers have proposed using approaches for paper-based adsorbent materials in terms of aerogels (Bi *et al*., 2014; Feng, Nguyen, Fan, & Duong, 2015; Han, Sun, Zheng, Li, & Jin, 2016). The chemical compositions of WP are presented in Table 1. Adsorbent aerogel is a light, porous material exhibiting many excellent properties in adsorption efficiency including transparency, extremely high porosity, large surface area, and high mechanical strength. One decade ago, aerogel was developed for heavy metal ion adsorption from contaminated water, environments, and biological systems (Nguyen *et al*., 2019). However, the adsorption capacity is quite low when directly used as WP aerogel adsorbent. Many improvement methods have been proposed including copolymer and homogeneity with high porosity material methods (Feng *et al*., 2015; Han *et al*., 2016). In Thailand, rice husk (RH) is generated annually as co-products from paddy fields and rice mills in large quantities. The study of Neamhom (2019) suggested that RH could help alleviate pollutants as an adsorptive material for ferrous ion, hardness, and nuisance. RH is mainly composed of 30.6 to 35.0% cellulose, 18.3 to 33.0% hemicellulose, 23.0 to 29.9% lignin, and 9.0 to 19.5% ash contents (Hoyos-Sánchez, Córdoba-Pacheco, Rodríguez-Herrera, & Uribe-Kaffure, 2017; Johar, Ahmad, & Dufresne, 2012). Presently more advantages for RH-based sorbent material have been discussed. Notably, expanding applications and techniques have mostly considered aqueous and some gaseous phases. This work aimed to investigate the use of various WP materials obtained from offices to remove emissions in terms of $PM_{2.5}$ and TVOC emitted from printing jobs so as to determine their adsorption capacity and behaviors. The results would constitute one method to reduce health risks from indoor air pollutant exposure emitted by printers.

2. Materials and Methods

2.1 Preparing aerogel adsorbent

WP used in this work consisted of 2-sided used paper (2P), color, and newspaper. They were collected from academic offices and smashed by automatic machine into small pieces. To remove impurities, they were further dispersed in a 0.5 M sodium hydroxide (NaOH) solution (1:20 w/v) at room temperature for 4 hours in permanent agitation on a 200-rpm shaker. Then they were washed with distilled water (DI), soaked in 0.5 M hydrochloric acid (HCl) solution (1:20 w/v) for 4 hours at a stirring speed of 200 rpm, and dried at 40 °C for 48 hours (Hoyos-Sánchez *et al*., 2017; Zhao *et al*., 2018). All chemicals were analytical reagent (AR) grade.

RH was collected from local paddy field and washed thoroughly with purified water several times to eliminate impurities. It was cleaned by soaking in 0.5 M HCl solution (1:20 w/v) at room temperature for 4 hours in permanent agitation on a 200 rpm shaker. Then RH was washed with distilled water and soaked in a 0.5 M NaOH solution (1:20 w/v) for 4 hours at the same conditions above (Kumar & Bandyopadhyay, 2006; Ndazi, Nyahumwa, & Tesha, 2008). Purified RH was repeatedly washed with distilled water and dried at 40 °C for 48 hours and sieved using a 60-mesh screen.

The experimental designs to prepare aerogel adsorbents are presented in Table 2. For each protocol, proportions of WP and RH were varied from one to two (4 and 8 grams, respectively). WP and RH were poured in 100 mL of NaOH/urea solution and stirred at 1,000 rpm for 10 minutes at room temperature. Then 100 mL 0.5 Methanol was added to the mixture and dried at room temperature for 24 hours. A homogenous mixture was obtained and further washed with DI water to obtain neutral pH. After that, the mixture was freeze dried to generate aerogel. Aerogel was obtained after freeze drying for 48 hours (Li *et al*., 2018a, 2018b).

2.2 Morphology characterizations

Aerogel morphologies were investigated using a scanning electron microscopy (SEM, FEI- Quanta 250). Before testing, the aerogel samples were kept dry before SEM. Then, cross-sections were sputter-coated with a thin layer of platinum before observing.

2.3 Batch adsorption experiments

Adsorbent aerogel materials were prepared for batch experiments using a 3x2x3 factorial design method. Independent variables included three types of WP (2P, color,

Table 1.   Chemical characteristics of wastepaper

Wastepaper	Percentage (%, w/w)					Reference
	Cellulose	Hemicellulose	Lignin	Ash	Others	
Office paper	-	-	1.4	23.4	-	Zhou *et al*. (2017)
	62.0	5.0	1.0	-	30.0	Ioelovich (2014)
	78.6	4.7	1.2	9.0	3.3	Guerfali *et al*. (2015)
Newspaper	-	-	10.3	15.2	-	Zhou *et al*. (2017)
	38.0	15.0	21.0	-	19.0	Ioelovich (2014)
	49.3	12.2	19.2	1.5	4.9	Guerfali *et al*. (2015)
Cardboard	-	-	13.1	12.5	-	Zhou *et al*. (2017)
	61.0	12.0	18.0	-	7.0	Ioelovich (2014)

Table 2. Experimental design and their average pore size diameter

Experiment	Wastepaper	Pretreatment	Proportion of rice husk	Pore size (µm)
E-1	2P	P	1 2P/P : 1 RH	28.166
E-2	2P	P	1 2P/P : 2 RH	29.058
E-3	2P	P	2 2P/P : 1 RH	40.450
E-4	2P	NP	1 2P/NP : 1 RH	38.080
E-5	2P	NP	1 2P/NP : 2 RH	30.210
E-6	2P	NP	2 2P/NP : 1 RH	38.888
E-7	Color	P	1 Color/P : 1 RH	42.900
E-8	Color	P	1 Color/P : 2 RH	53.250
E-9	Color	P	2 Color/P : 1 RH	43.452
E-10	Color	NP	1 Color/NP : 1 RH	44.916
E-11	Color	NP	1 Color/NP : 2 RH	24.372
E-12	Color	NP	2 Color/NP : 1 RH	26.620
E-13	WNP	P	1 WNP/P : 1 RH	42.076
E-14	WNP	P	1 WNP/P : 2 RH	35.492
E-15	WNP	P	2 WNP/P : 1 RH	31.700
E-16	WNP	NP	1 WNP/NP : 1 RH	55.340
E-17	WNP	NP	1 WNP/NP : 2 RH	43.388
E-18	WNP	NP	2 WNP/NP : 1 RH	24.096

Remarks: The "P" is pretreatment process while "NP" is no pretreatment process

and newspaper), two types of pretreatment process (with pretreatment and without pretreatment), and three proportion for RH and WP (1:1, 1:2, and 2:1). Gaseous samples were collected using a study chamber as presented in Figure 1. The inner volume was about 0.08 m³ (59 cm x 33 cm x 40 cm). This reactor was constructed using cardboard material. During experiments, the average temperature and humidity were measured in a range between 25±2 °C and 38 to 40%, respectively. Each test was performed using a laser printer (Brother HL-2130 series) with a printing speed of 20 pages/minutes and about 30 pages in a continuous printing process. The DustTrak II Aerosol Monitor (1.52 L/min flow rate) with $PM_{2.5}$ selective cyclone and the MiniRAE 3000 PID were employed after printing 10 minutes to monitor the real time mass concentration of $PM_{2.5}$ and TVOC, respectively. All aerogel were performed in the desiccator before assess the experiment. All experiments were conducted in triplicate.

2.4 Calculations

Removal efficiency (RE) and adsorption capacity (Q_t) for $PM_{2.5}$ and TVOC were calculated using Equation (1) and (2), respectively.

$$RE = \frac{X_0 - X_1}{X_0} \times 100 \qquad (1)$$

$$Q_t = \frac{(C_0 - C_e) \times V_d}{M_b} \qquad (2)$$

X_0 represents the mass pollutant concentration without aerogel adsorbent added and X_1 is the residual mass pollutant concentration after contact with the aerogel adsorbent. Q_t represents the pollutant concentration adsorbed onto the surface of aerogel adsorbents (mg/g and ppm/g for $PM_{2.5}$, and TVOC, respectively), C_0 is the initial or

background pollutant concentration in the experimental setup (mg/m³ and ppm for $PM_{2.5}$ and TVOC, respectively), C_e is the mass pollutant concentration at equilibrium (mg/m³ and ppm for $PM_{2.5}$ and TVOC, respectively), V_d is the volume of solution (0.08 m³) and M_b is the amount of adsorbent (1 gram).
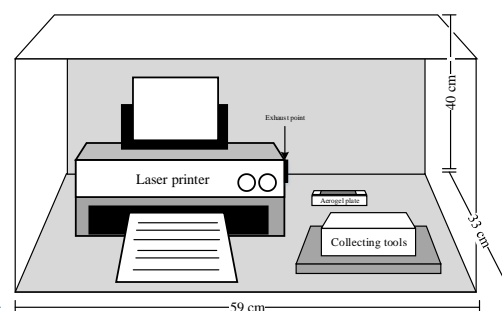

Figure 1. Experimental setup

2.5 Adsorption isotherms

To describe the relationship between the number of pollutants adsorbed and the remaining pollutant concentration in the experiments at equilibrium, adsorption isotherm studies were conducted using the same initial gaseous concentration in a chamber presented in Figure 1. Amount of aerogel adsorbent was varied from 2 to 6 grams. Appropriate adsorbent was tested for its ability to adsorb the pollutant concentration. Results were plotted in two-parameter sorption isotherm models, i.e., the Langmuir and Freundlich models. Langmuir isotherm was used to determine the adsorption behavior on the surface of the adsorbent on the monolayer and equivalent sites on the surface while the latter model was based on multilayer adsorption with a heterogeneous surface (Freundlich, 1906; Langmuir, 1918). They were expressed mathematically using Equation (3) and (4), respectively.

$$q_e = \frac{q_{max} K_L C_e}{(1 + K_L C_e)} \tag{3}$$

$$q_e = K_F C_e^n \tag{4}$$

where q_e is adsorption capacity at equilibrium which represents the pollutant concentration adsorbed onto the surface of aerogel adsorbents (mg/g and ppm/g for PM2.5, and TVOC, respectively), C_0 is the initial or background pollutant concentration in the experimental setup (mg/g and ppm/g for PM2.5, and TVOC, respectively), q_{max} is the adsorption capacity of the adsorbent at equilibrium (mg/g or ppm/g) in the homogeneous layer, K_L is the Langmuir isotherm constant, C_e is concentration at equilibrium, K_F is the Freundlich equilibrium constant, and n is an affinity constant between the adsorbates and the adsorbents. In the sense of control; n greater than one implies stronger interaction between an adsorbent and metallic ion (Bang & Kim, 2017; Nikiforova & Kozlov, 2016; Porubska, Jomová, & Branisa, 2021).

3. Results and Discussion

3.1 Characterizations of aerogel adsorbent

Microstructures of aerogel adsorbents produced from wastepaper and rice husk are shown in Figure 2. Each experiment showed various fiber sheet structures in the lateral fiber dimension. The dimension network structure presented a pore size diameter from 24.1 – 55.3 µm as detailed in Table 2.
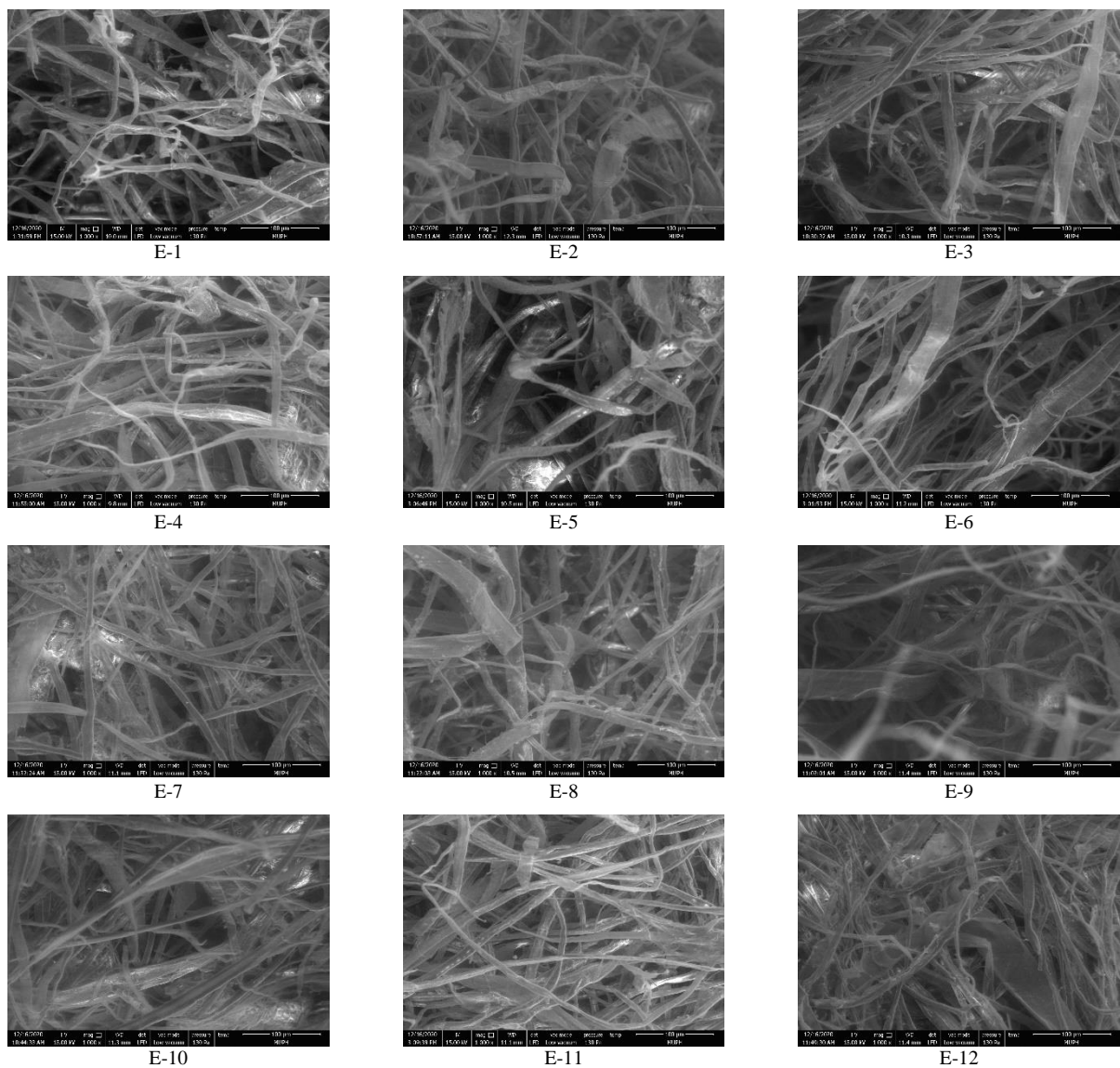

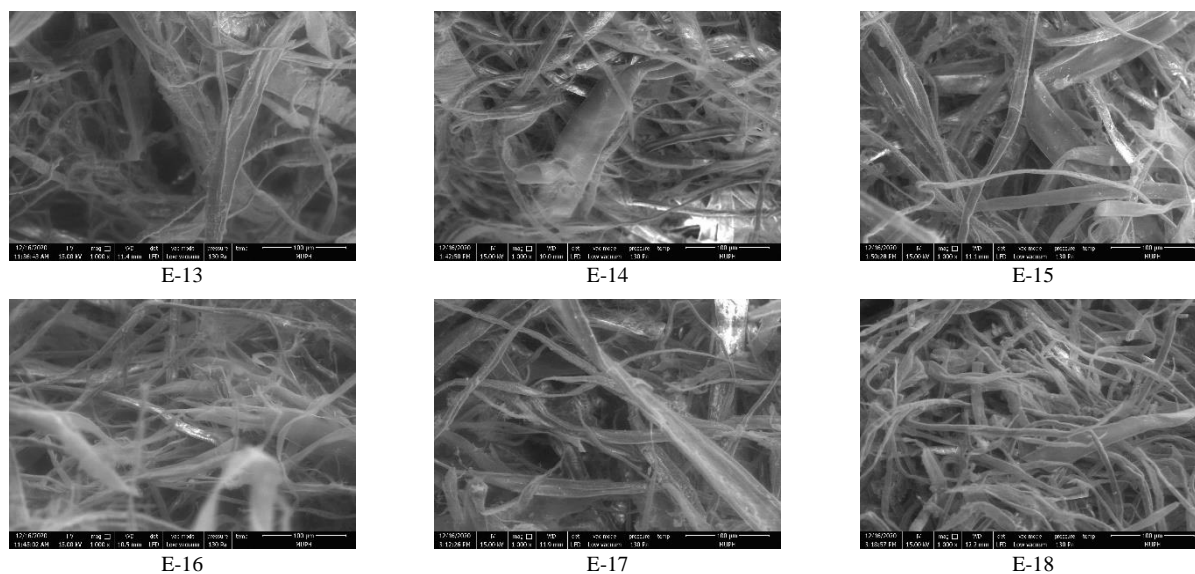Figure 2.   SEM micrographs of aerogel adsorbents

E-13   E-14   E-15

E-16   E-17   E-18

Figure 2.   Continued.

3.2 Emissions concentration from printing jobs

The incomplete toner transfer between the charged drum and the paper surface is accounted for as the main cause for particulate emission (Lee, Lam, & Fai, 2001). The study of Lee and Hsu (2007) conducted at 12 photocopy centers in Taiwan reported that indoor $PM_{2.5}$ increased during the operation of photocopy machines about 10 to 83 $\mu g/m^3$ corresponding to the survey in Germany (Salthammer, Schripp, Uhde, & Wensing, 2012). In this study, concentrations of $PM_{2.5}$, measured during operation modes of laser printers, was found at 0.019 ± 0.005 mg/m^3. This finding was lower than the acceptable standard for respirable particulates by ASHRAE standard 62-2004 and DOSH of 0.15 mg/m^3. On the other hand, during the COVID-19 pandemic, the occurrence of indoor particulate matter in terms of $PM_{2.5}$ may create a potential risk for the transmission of SARS-CoV-2 in offices and other indoor environments with high user occupancy (He & Han, 2020). Measurements were also conducted regarding TVOC while printing resulting in concentrations of 0.185 ± 0.005 ppm. This value can comparable to one related work (Damanhuri, Leman, Abdullah, & Hariri, 2015). The acceptable limit of indoor TVOC (3 ppm) (Department of Occupational Safety and Health, DOSH, 2005) was below standard. In contrast, the study of Afshar-mohajer, Wu, Ladun, & Rajon (2015) revealed health effects due to exposure to high VOCs included breathing problems, eye irritation, headache, respiratory illness and cancer. However, in terms of control and toxicology, they confirmed negative effects in terms of both acute and chronic conditions to human health (Thongchom, On-si, Puongphan, Chumprasittichok, & Neamhom, 2021).

3.3 Aerogel adsorbents and their removal efficiency

Microstructures of aerogel adsorbents produced from WP and RH showed various pore size diameters as shown in Table 2. The dimension network structure presented a pore size diameter from minimum to maximum of 28.2 to 38.9, 24.4 to 53.3, and 24.1 to 55.3 μm for experiments of 2P-RH, color-RH, and WNP-RH, respectively. The properties of aerogel pore size diameters are linked to pollutants adsorption kinetics due to the small micropores creating a higher portion of adsorbent reactive areas (Suresh *et al*., 2019; Witoon & Chareonpanich, 2012). Hence, it could imply that 2P would create the best action regarding adsorption effects. At the existing conditions of the experiment, the percentage of removal efficiency and their adsorption capacity are interpreted in Table 3. For $PM_{2.5}$, a highest efficiency was produced with E-8, E-16, and E-17 with final $PM_{2.5}$ concentration less than 0.008 mg/L. The performances of adsorption capacity ranged from 1.0 to 1.6 $\mu g/g$. Among these values, the means and standard deviations (SD.) were found of 1.28 ± 0.15, 1.33 ± 0.12, and 1.42 ± 0.13 $\mu g/g$ for experimental preparations of 2P-RH, color-RH, and WNP-RH, respectively. However, peak TVOC capturing was found in E-9 at 67.0% and 0.0159 mg/g, followed by E-12, E-11, and E-4, in rank. The mean$\pm$SD. ($\mu g/g$) of adsorption capacity for 2P-RH, color-RH, and WNP-RH were calculated to be 8.14 ± 5.28, 8.88 ± 6.90, and 3.21 ± 2.78, respectively.

### 3.3.1 Reduction potential from 2P-RH

Figure 3(a), the emission of $PM_{2.5}$ adsorbed by 2P-RH (E-1 to E-6) was equivalent to about one half total reduction and slightly worse in E-6. E-2 and E-3 presenting the same value of final $PM_{2.5}$ concentration of 0.008 mg/l. Figure 3(b) exhibits the similar tendency by E-4 for final concentration of TVOC (0.081 ppm). Moreover, E-6 demonstrated a lower finishing concentration, compared with E-4. In summary, E-4 exhibited superior help in capturing and reducing both of the emissions from printing jobs.

### 3.3.2 Reduction potential from color-RH

A decreasing value of emissions was found in a cluster of color-RH (E-7 to E-12). For $PM_{2.5}$, the slightly better values of less than 0.008 mg/l were found from E-7,

Table 3. Removal efficiency and adsorption capacity performances of aerogel adsorbents

| Experiment	Description	Removal efficiency (%)		Adsorption capacity (mg/g)	
		PM2.5	TVOC	PM2.5	TVOC
E-1	2P/P/1:1	52.6	15.1	0.0013	0.0036
E-2	2P/P/1:2	57.9	23.8	0.0014	0.0057
E-3	2P/P/2:1	57.9	26.5	0.0014	0.0063
E-4	2P/NP/1:1	52.6	56.2	0.0013	0.0135
E-5	2P/NP/1:2	52.6	16.8	0.0013	0.0040
E-6	2P/NP/2:1	42.1	67.0	0.0010	0.0161
E-7	Color/P/1:1	57.9	9.2	0.0014	0.0022
E-8	Color/P/1:2	63.2	21.1	0.0015	0.0050
E-9	Color/P/2:1	42.6	67.0	0.0013	0.0159
E-10	Color/NP/1:1	57.9	4.3	0.0014	0.0010
E-11	Color/NP/1:2	47.4	56.8	0.0012	0.0136
E-12	Color/NP/2:1	47.4	64.9	0.0012	0.0156
E-13	WNP/P/1:1	57.9	2.7	0.0014	0.0006
E-14	WNP/P/1:2	57.9	4.9	0.0014	0.0011
E-15	WNP/P/2:1	47.4	2.7	0.0012	0.0006
E-16	WNP/NP/1:1	63.2	17.3	0.0016	0.0041
E-17	WNP/NP/1:2	63.2	29.2	0.0015	0.0069
E-18	WNP/NP/2:1	57.9	24.3	0.0014	0.0058
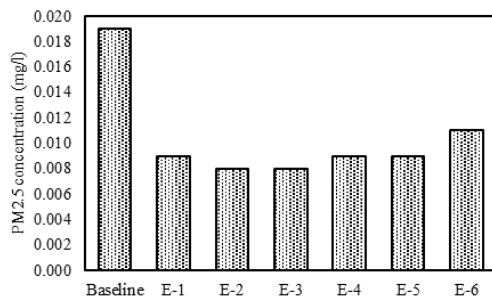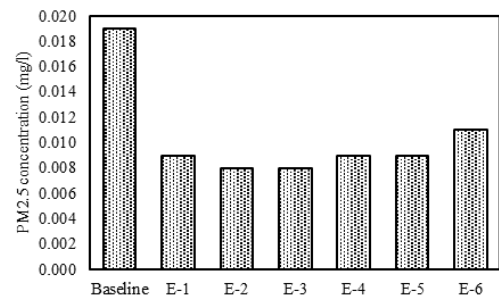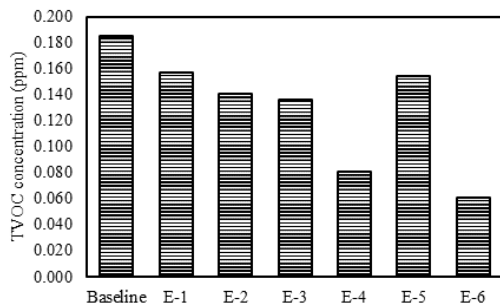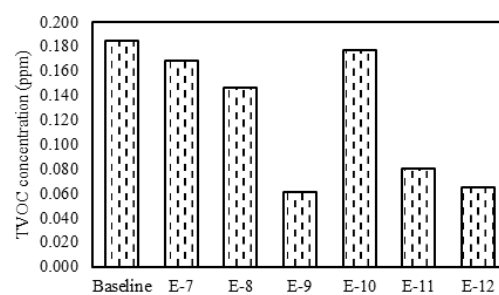
Figure 3. Emission concentrations after 2P-RH experiments; (a) PM2.5 and (b) TVOC

Figure 4. Emission concentrations after color-RH experiments; (a) PM2.5 and (b) TVOC

E-8, and E-10 as presented in Figure 4. On the other hand, final TVOC concentration obtained in E-7, E-8, and E-10 was near the baseline value. However, based on the unsuitable of adsorption amount, the single use of aerogel adsorbent from color paper and RH was not suitable for PM2.5 and TVOC.

3.3.3 Reduction potential from WNP-RH

Similar to the reduction potential from color-RH aerogel, the final concentration of TVOC in E-13 to E-18

was near the existing ones as illustrated in Figure 5. Differences from TVOC and PM2.5 concentration obtained from this aerogel were comparable to two other aerogels due to their total half reduction with final value less than 0.008 mg/l except E-15 (0.010 mg/l).

3.4 Adsorption isotherm models

Based on the best adsorption results from related sections, the fourth experiments (2P/NP/1 2P/NP:1 RH) were
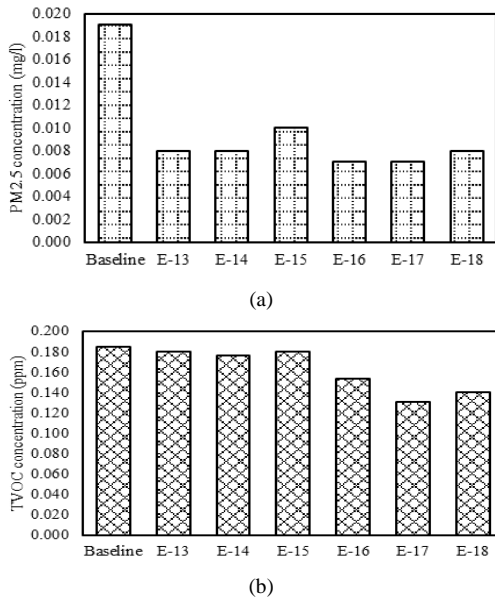
(a)

(b)

Figure 5. Emission concentrations after WNP-RH experiments; (a) PM2.5 and (b) TVOC

further used to describe the adsorption behavior and determine their interactions between pollutants and aerogel adsorbent. Freundlich and Langmuir isotherm models were used to explain the performance between the two-parameter sorption conditions. Figure 6(a) and (c) shows the linear curve for log qe against log Ce values whereas the plotting of 1/qe versus 1/Ce values is presented in Figures 6(b) and 6(c). The Freundlich isotherm models offered correlation coefficient values (R^2) of 0.6686 and 0.9770 for $PM_{2.5}$ and TVOC, respectively. However, the coefficient of correlation from the Langmuir model was found to be 0.8201 and 0.9973 for $PM_{2.5}$ and TVOC, respectively. The value of R^2 indicated the compliance of the experimental data with the isotherm models (Li *et al.*, 2017). Moreover, the R^2 value higher than 0.95 indicated that the exponential adsorption data fit well in the model (Nguyen *et al.*, 2019). Hence, these indicated that the Langmuir isotherm model was adequate in describing the relationship between adsorption capacity and their saturated concentration. Similar to related works on the adsorption of heavy metal ions using aerogel adsorbent (Li, Jia, Ni, & Li, 2017; Li *et al.*, 2018a), the linearity of Langmuir plots for both $PM_{2.5}$ and TVOC suggested strong bonding involving chemical forces between aerogel adsorbent and pollutants. Results also suggested that the mechanism of emissions uptake was the monolayer homogeneous adsorption process on the surface of the adsorbent (Saleh & Danmaliki, 2016; Trakoolsa & Yoochatchaval, 2020). Isotherm parameters and correlation coefficient from both Langmuir and Freundlich models are summarized in Table 4. Based on the Langmuir isotherm, the saturated adsorption capacity of $PM_{2.5}$ and TVOC were calculated to be 0.8 mg/mg and 9.9 ppm/mg, respectively.

4. Conclusions

The use of synthesized adsorbent aerogel from WP and RH may offer several benefits for emission control in
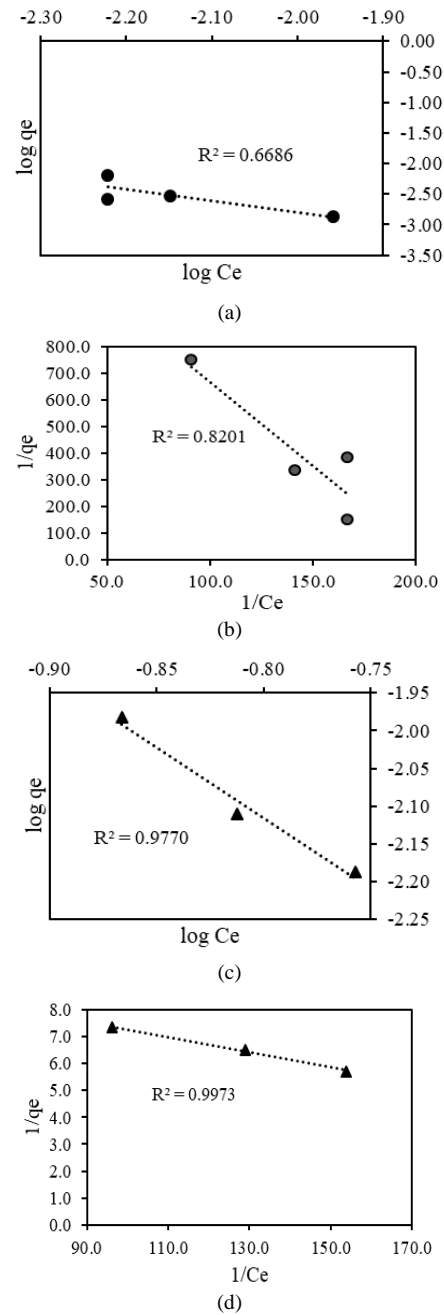

(a)

(b)

(c)

(d)

Figure 6. Adsorption isotherm models, (a) Freundlich-PM2.5; (b) Langmuir-PM2.5; (c) Freundlich-TVOC; (d) Langmuir-TVOC

working area environments and reduce the risk of exposure for indoor air pollutants such as $PM_{2.5}$ and TVOC. RH and three types of office WP including 2-sided used paper; 2P, color, and newspaper were used as raw materials to produce aerogel adsorbent by 18 factorial design experiments. In the experiments, the initial concentrations of $PM_{2.5}$ and TVOC from printing jobs were measured at 0.019±0.005 mg/m³ and 0.185±0.005 ppm, respectively. From this finding, all experiments demonstrated the efficiency in adsorption of $PM_{2.5}$ with removal percentages of 42.1 to 63.2%. Contrasting

Table 4.　Isotherm parameters for PM2.5 and TVOC adsorptions on aerogel adsorbents

Isotherm model	Emissions	Estimated isotherm parameters				
		q_{max} (mg, ppm/g)	K_L	K_F	n	R^2
Freundlich	PM2.5	-	-	0.0015	-0.16	0.6686
	TVOC	-	-	-0.0272	-0.54	0.9770
Langmuir	PM2.5	0.0008	-3.34	-	-	0.8201
	TVOC	0.099	-356.93	-	-	0.9973

with the efficiency for PM2.5, only some experiments proposed a reduced value for final TVOC concentration. Based on these results, only the best fit trial for both PM2.5 and TVOC of 2P was further used to determine their adsorption isotherm. At equilibrium, the sample fitted the Langmuir model well with correlation coefficient (R^2) of 0.8201 and 0.9973 for PM2.5 and TVOC, respectively. It implied that the adsorption sites on the surface of the aerogel adsorbent produced from 2P/NP/1 2P/NP: 1RH conditions were homogeneous in nature. The optimum adsorption capacity for PM2.5 and TVOC was 0.0008 mg/g and 0.099 ppm/g, respectively. Furthermore, these conversions constituted effective reuse approaches for WP and RH with low cost, environmental friendliness, and excellence in adsorption capacity.

Acknowledgments

References

Afshar-mohajer, N., Wu, C., Ladun, T., & Rajon, D. A. (2015). Characterization of particulate matters and total VOC emissions from a binder jetting 3D printer. *Building and Environment*, *93*, 293–301. doi:10.1016/j.buildenv.2015.07.013

Bang, S. Y., & Kim, J. H. (2017). Isotherm, kinetic, and thermodynamic studies on the adsorption behavior of 10-deacetylpaclitaxel onto Sylopute. *Biotechnology and Bioprocess Engineering*, *22*(5), 620–630. doi:10.1007/s12257-017-0247-4

Bi, H., Huang, X., Wu, X., Cao, X., Tan, C., & Yin, Z. (2014). Carbon microbelt aerogel prepared by waste paper: an efficient and recyclable sorbent for oils and organic solvents. *Small*, *10*, 3544–3550. doi:10.1002/smll.201303413

Chullasuk, P., Chapman, R. S., & Taneepanichskul, N. (2016). The association between respirable dust exposure and allergic symptoms in the libraries and general offices at Chulalongkorn University, Bangkok, Thailand. *Songklanakarin Journal of Science and Technology*, *38*(4), 407–412. doi:10.14456/sjst-psu.2016.53

Damanhuri, A. A. M., Leman, A. M., Abdullah, A. H., & Hariri, A. (2015). Effect of toner coverage percentage and speed of laser printer on Total Volatile Organic Compound (TVOC). *Chemical Engineering Transactions*, *45*, 1381–1386. doi:10.3303/CET1545231

Department of Occupational Safety and Health. (2005). Code of practice on indoor air quality.

Feng, J., Nguyen, S. T., Fan, Z., & Duong, H. M. (2015). Advanced fabrication and oil absorption properties of super-hydrophobic recycled cellulose aerogels. *Chemical Engineering Journal*, *270*, 168–175. doi:10.1016/j.cej.2015.02.034

Freundlich H. (1906). Uber die adsorption in losungen. *Zeitschrift Fur Physikalische Chemie*, *54*, 385–470.

Gu, J., & Karrasch, S. (2020). Review of the characteristics and possible health effects of particles emitted from laser printing devices. *Indoor Air*, *30*(October 2019), 396–421. doi:10.1111/ina.12646

Guerfali, M., Saidi, A., & Gargouri, A. (2015). Enhanced enzymatic hydrolysis of waste paper for ethanol production using separate saccharification and fermentation. *Applied Biochemistry and Biotechnology*, *175*(1), 25–42. doi:10.1007/s12010-014-1243-1

Han, S., Sun, Q., Zheng, H., Li, J., & Jin, C. (2016). Green and facile fabrication of carbon aerogels from cellulose-based waste newspaper for solving organic pollution. *Carbohydrate Polymers*, *136*, 95–100. doi:10.1016/j.carbpol.2015.09.024

He, C., Morawska, L., & Taplin, L. (2007). Particle emission characteristics of office printers. *Environmental Science and Technology*, *41*(17), 6039–6045. doi:10.1021/es063049z

He, S., & Han, J. (2020). Electrostatic fine particles emitted from laser printers as potential vectors for airborne transmission of COVID - 19. *Environmental Chemistry Letters*, *7*, 1–8. doi:10.1007/s10311-020-01069-8

Hoyos-Sánchez, M. C., Córdoba-Pacheco, A. C., Rodríguez-Herrera, L. F., & Uribe-Kaffure, R. (2017). Removal of Cd (II) from aqueous media by adsorption onto chemically and thermally treated rice husk. *Journal of Chemistry*, *2017*. doi:10.1155/2017/5763832

Ioelovich, M. (2014). Waste paper as promising feedstock for production of biofuel. *Journal of Scientific Research and Reports*, 3(7), 905–916.

Johar, N., Ahmad, I., & Dufresne, A. (2012). Extraction, preparation and characterization of cellulose fibres and nanocrystals from rice husk. *Industrial Crops*

and Products, *37*(1), 93–99. doi:10.1016/j.indcrop. 2011.12.016

Kagi, N., Fujii, S., Horiba, Y., Namiki, N., & Ohtani, Y. (2007). Indoor air quality for chemical and ultrafine particle contaminants from printers. *Building and Environment*, *42*, 1949–1954. doi:10.1016/j.build env.2006.04.008

Kumar, U., & Bandyopadhyay, M. (2006). Sorption of cadmium from aqueous solution using pretreated rice husk. *Bioresource Technology*, *97*(1), 104–109. doi:10.1016/j.biortech.2005.02.027

Langmuir, I. (1918). The adsorption of gases on plane surfaces of glass, mica and platinum. *The Journal of the American Chemical Society*, *40*(9), 1361–1403.

Lee, C., Dai, Y., Chien, C., & Hsu, D. (2006). Characteristics and health impacts of volatile organic compounds in photocopy centers. *Environmental Research*, *100*, 139–149. doi:10.1016/j.envres.2005.05.003

Lee, C., & Hsu, D. (2007). Measurements of fine and ultrafine particles formation in photocopy centers in Taiwan. *Atmospheric Environment*, *41*(31), 6598–6609. doi:10.1016/j.atmosenv.2007.04.016

Lee, J., & Koo, J.-W. (2015). Occupational diseases among office workers and prevention strategies. *Journal of the Ergonomics Society of Korea*, *34*(2), 125–134. doi:10.5143/jesk.2015.34.2.125

Lee, S. ., Lam, S., & Fai, H. K. (2001). Characterization of VOCs, ozone, and PM10 emissions from office equipment in an environmental chamber. *Building and Environment*, *36*(7), 837–842.

Li, W. C., Law, F. Y., & Chan, Y. H. M. (2017). Biosorption studies on copper (II) and cadmium (II) using pretreated rice straw and rice husk. *Environmental Science and Pollution Research*, *24*(10), 8903–8915. doi:10.1007/s11356-015-5081-7

Li, W., Khalid, H., Amin, F. R., Zhang, H., Dai, Z., Chen, C., & Liu, G. (2020). Biomethane production characteristics, kinetic analysis, and energy potential of different paper wastes in anaerobic digestion. *Renewable Energy*, *157*, 1081–1088. doi:10. 1016/j.renene.2020.04.035

Li, Z., Jia, Z., Ni, T., & Li, S. (2017). Adsorption of methylene blue on natural cotton based fl exible carbon fi ber aerogels activated by novel air-limited carbonization method. *Journal of Molecular Liquids*, *242*, 747–756. doi:10.1016/j.molliq.2017. 07.062

Li, Z., Shao, L., Hu, W., Zheng, T., Lu, L., Cao, Y., & Chen, Y. (2018a). Excellent reusable chitosan / cellulose aerogel as an oil and organic solvent absorbent. *Carbohydrate Polymers*, *191*(February), 183–190. doi:10.1016/j.carbpol.2018.03.027

Li, Z., Shao, L., Ruan, Z., Hu, W., Lu, L., & Chen, Y. (2018b). Converting untreated waste office paper and chitosan into aerogel adsorbent for the removal of heavy metal ions. *Carbohydrate Polymers*, *193*(March), 221–227. doi:10.1016/j.carbpol.2018. 04.003

Lovskaya, D., Menshutina, N., Mochalova, M., & Nosov, A. (2020). Chitosan-based aerogel particles as highly effective local hemostatic agents. Production

process and in vivo evaluations. *Polymers*, *12*(9), 2055. doi:10.3390/polym12092055

Ndazi, B. S., Nyahumwa, C., & Tesha, J. (2008). Chemical and thermal stability of rice husks against alkali treatment. *BioResources*, *3*(4), 1267–1277. doi:10. 15376/biores.3.4.1267-1277

Neamhom, T. (2019). Use of agricultural residues to remove iron from groundwater in modified airlift aerator. *Environment and Natural Resources Journal*, *17*(3), 58–67. doi:10.32526/ennrj.17.3.2019.23

Nguyen, T. T., Ma, H. T., Avti, P., Bashir, M. J. K., Ng, C. A., Wong, L. Y., & Tran, N. Q. (2019). Adsorptive removal of iron using SiO2 nanoparticles extracted from rice husk ash. *Journal of Analytical Methods in Chemistry*, *2019*, 1–9. doi:10.1155/2019/6210240

Nikiforova, T. E., & Kozlov, V. A. (2016). Regularities of the effects of the nature of polysaccharide materials on distribution of heavy metal ions in a heterophase biosorbent–water solution system. *Protection of Metals and Physical Chemistry of Surfaces*, *52*(3), 243-271. doi:10.1134/S2070205116030217

Porubska, M., Jomová, K., & Branisa, J. (2021). Analysis of natural materials' adsorption efficiency relating co(ii) using atomic absorption spectroscopy: laboratory experiment. *Journal of Chemical Education*, *98*(2), 626–632. doi:10.1021/acs. jchemed.0c00210

Rinki, K., Dutta, P. K., Hunt, A. J., MacQuarrie, D. J., & Clark, J. H. (2011). Chitosan aerogels exhibiting high surface area for biomedical application: preparation, characterization, and antibacterial study. *International Journal of Polymeric Materials and Polymeric Biomaterials*, *60*(12), 988–999. doi:10.1080/00914037.2011.553849

Saleh, T. A., & Danmaliki, G. I. (2016). Adsorptive desulfurization of dibenzothiophene from fuels by rubber tyres-derived carbons: Kinetics and isotherms evaluation. *Process Safety and Environmental Protection*, *102*, 9–19. doi:10. 1016/j.psep.2016.02.005

Salthammer, T., Schripp, T., Uhde, E., & Wensing, M. (2012). Aerosols generated by hardcopy devices and other electrical appliances. *Environmental Pollution*, *169*, 167–174. doi:10.1016/j.envpol.2012.01.028

Shi, X., Chen, R., Huo, L., Zhao, L., Bai, R., & Long, D. (2015). Evaluation of nanoparticles emitted from printers in a clean chamber, a copy center and office rooms: health risks of indoor air quality. *Journal of Nanoscience and Nanotechnology*, *15*(February 2016), 9554–9564. doi:10.1166/jnn.2015.10314

Suresh, P., Korving, L., Keesman, K. J., Loosdrecht, M. C. M. Van, & Witkamp, G. (2019). Effect of pore size distribution and particle size of porous metal oxides on phosphate adsorption capacity and kinetics. *Chemical Engineering Journal*, *358*(September 2018), 160–169. doi:10.1016/j.cej.2018.09.202

Thongchom, T., On-si, N., Puongphan, C., Chumprasittichok, T., & Neamhom, T. (2021). Health risks from indoor PM10 and effects of sick building syndrome in office workers. *Thai Journal of Public Health*, *51*(2), 170–180.

Trakoolsa, O., & Yoochatchaval, W. (2020). Adsorption efficiency of copper and nickel by activated carbon from coffee ground. *EnvironmentAsia*, *13*, 46–53. doi:10.14456/ea.2020.21

United State Environmental Protection Agency (1997). An office building occupant's guide to indoor air quality. Retrieved from https://www.epa.gov/sites/ production/files/2014-08/documents/occupants_ guide.pdf

Witoon, T., & Chareonpanich, M. (2012). Effect of pore size and surface chemistry of porous silica on CO2 adsorption. *Songklanakarin Journal of Science and Technology*, *34*(4), 403–407.

Zhao, X., Zeng, X., Qin, Y., Li, X., Zhu, T., & Tang, X. (2018). An experimental and theoretical study of the adsorption removal of toluene and chlorobenzene on coconut shell derived carbon. *Chemosphere*, *206*, 285–292. doi:10.1016/j.chemosphere.2018.04.126

Zhou, W., Gong, Z., Zhang, L., Liu, Y., Yan, J., & Zhao, M. (2017). Feasibility of lipid production from waste paper by the oleaginous yeast cryptococcus curvatus. *BioResources*, *12*(3), 5249–5263. doi:10.15376/biores.12.3.5249-5263